Microbial assemblages associated with the invasive kelp Undaria pinnatifida in patagonian coastal waters: Structure and alginolytic potential

Mariana Lozada, María Soledad Zabala, Patricia E. García, María C. Diéguez, Gregorio Bigatti, Paulina Fermani, Fernando Unrein, Hebe M. Dionisi

PII: S0048-9697(22)01722-3

DOI: https://doi.org/10.1016/j.scitotenv.2022.154629

Reference: STOTEN 154629

To appear in: *Science of the Total Environment*

Received date: 5 January 2022

Revised date: 12 March 2022

Accepted date: 13 March 2022

Please cite this article as: M. Lozada, M.S. Zabala, P.E. García, et al., Microbial assemblages associated with the invasive kelp Undaria pinnatifida in patagonian coastal waters: Structure and alginolytic potential, *Science of the Total Environment* (2021), https://doi.org/10.1016/j.scitotenv.2022.154629

Microbial assemblages associated with the invasive kelp *Undaria pinnatifida* in patagonian coastal waters: structure and alginolytic potential

Mariana Lozada[1*], María Soledad Zabala[2], Patricia E. García[3], María C. Diéguez[3], Gregorio Bigatti[2,4], Paulina Fermani[1], Fernando Unrein[5,6], Hebe M. Dionisi[1]

[1]Laboratorio de Microbiología Ambiental (CESIMAR-CONICET/IBIOMAR-CONICET), Puerto Madryn, Argentina

[2]Laboratorio de Reproducción y Biología Integrativa de Invertebrados Marinos (IBIOMAR-CONICET), Puerto Madryn, Argentina

[3]Grupo de Ecología de Sistemas Acuáticos a Escala de Paisaje (GESAP, INIBIOMA-CONICET-UNComa), Bariloche, Argentina

[4]Universidad Espíritu Santo, Ecuador

[5]Laboratorio de Ecología y Fotobiología Acuática, Instituto Tecnológico de Chascomús (CONICET-UNSAM), Chascomús, Argentina

[6]Escuela de Bio y Nanotecnologías (UNSAM), Argentina.

*Corresponding author. Instituto de Biología de Organismos Marinos (IBIOMAR-CONICET), Bvd. Brown 2915, U9120, Puerto Madryn, Chubut province, Argentina. e-mail: lozada@cenpat-conicet.gob.ar

Acknowledgements

All authors are staff members of The Argentinean National Research Council (CONICET). We gratefully thank María Victoria Quiroga for the technical assistance on the flow cytometer. This work was supported by ANPCyT (Grants PICT-2016-2101, PICT-2018-0969, and PICT-2018-0903).

Highlights

- Invasive kelp *U. pinnatifida* reshapes coastal environments in Patagonia
- Kelp senescence enhances DOC, POC and nutrients, impacting associated communities
- Kelp forest holds distinct epiphytic and free-living microbial assemblages
- Epiphytic and bottom seawater microbes have a key role in algal-derived DOM breakdown
- Specialized populations in epiphytic biofilms show the highest alginate-degrading potential

Abstract

Undaria pinnatifida is a brown algae native to Asia that has settled in various regions worldwide, periodically contributing with large quantities of C and nutrients during its annual cycle. In this work, we analyzed a coastal site in Patagonia (Argentina) that has been colonized for three decades by *U. pinnatifida*, focusing on associated microbial communities in three different compartments. An important influence of algae was observed in seawater, especially in the bottom of the algal forest during the austral summer (January) at the moment of greater biomass release. This was evidenced by changes in DOC concentration and its quality indicators (higher freshness and lower

humification index) and higher DIC. Although maximum values of NH_4 and PO_4 were observed in January, bottom water samples had lower concentrations than surface water, suggesting nutrient consumption by bacteria during algal DOM release. Concomitantly, bacterial abundance peaked, reaching $4.68 \pm 1.33 \times 10^5$ cells mL^{-1} (January), showing also higher capability of degrading alginate, a major component of brown algae cell walls. Microbial community structure was influenced by sampling date, season, sampling zone (surface or bottom), and environmental factors (temperature, salinity, pH, dissolved oxygen, nutrients). Samples of epiphytic biofilms showed a distinct community structure compared to seawater, lower diversity, and remarkably high alginolytic capability, suggesting adaptation to degrade algal biomass. A high microdiversity of populations of the genus *Leucothrix* (Gammaproteobacteria, Thiotrichales) that accounted for a large fraction of epiphytic communities was observed, and changed over time. Epiphytic assemblages shared more taxa with bottom than with surface seawater assemblages, indicating a certain level of exchange between communities in the forest surroundings. This work provides insight into the impact of *U. pinnatifida* decay on seawater quality, and the role of microbial communities on adapting to massive biomass inputs through rapid DOM turnover.

Introduction

The colonization and rapid spread of the brown alga *Undaria pinnatifida* in Patagonian coastal waters is a notable example of biological invasion. This kelp is native to Asia and has settled in coastal environments worldwide, facilitated by maritime transport and the presence of artificial structures (Epstein and Smale 2017; South et al. 2017). It has been listed along with the macroalga *Caulerpa taxifolia* in the Invasive Species Specialist Group list, which includes the 100 most

invasive species in the world (Epstein and Smale 2017). *U. pinnatifida* sporophytes form dense forests in shallow waters, reshaping the environment through changes in beach hydrodynamics, community structure, primary productivity and trophic interactions with cascading ecological effects (Casas et al. 2004; Irigoyen et al. 2011). In Argentina, this kelp has spread throughout patagonian coasts and beyond, covering almost 10° of latitude since its first record in 1992, and becoming an additional source of biomass in invaded environments (Rechimont et al. 2013; Dellatorre et al. 2014). Every year, *U. pinnatifida* stands yield high biomass, contributing with particulate and dissolved organic matter (POM and DOM, respectively) through exudation and erosion during its life cycle and decay at the end of summer (Bunicontro et al. 2019).

Coastal habitats dominated by kelps display a complex biogenic structure, exhibiting high primary production and biomass accumulation that influence environmental conditions for associated communities. A fraction of the primary production is readily consumed and processed, but in general most productivity enters detrital pathways, constituting a relevant energy source within coastal food webs and providing a trophic link between spatially disconnected habitats due to exports (Krause-Jensen and Duarte 2016, Smale et al. 2021). Natural and cultivated kelp forests are known to provide large amounts of detritus into the ecosystem, from eroding fronds, from the fragmentation and dislodgement of fronds and from senescence (Duarte et al. 2017; Pedersen et al. 2020; Fieler et al. 2021). Subsidies of these organic materials impact the surrounding environment or are exported to distant areas with consequences for C turnover and for the ecosystem (Smale et al. 2021). A large fraction of macroalgae debris settles into the sediments and another fraction remains in the water column enhancing the pelagic pools of POM and DOM (Krumhansl and Scheibling 2012; Wada and Hama 2013; Pedersen et al. 2020; Watanabe et al. 2020; Weigel and Pfister 2021). Microorganisms use these fractions in turn as a substrate for their growth (Hardison et al. 2010; Krumhansl and Scheibling 2012; Krause-Jensen and Duarte 2016; Smale et al. 2021).

Polysaccharides constitute a major fraction of brown algae biomass (Deniaud-Bouët et al. 2014). They are mostly labile to bacteria that can assimilate them through the expression of specific enzymes, transport systems and transcriptional regulators, thus playing a key role in their degradation and transference of C and nutrients into coastal food webs (Egan et al. 2013; Matos et al. 2016; Gobet et al. 2018; Arnosti et al. 2021). Polysaccharide-degrading bacteria can be found in sediments and seawater, however they are also associated with algae forming epiphytic biofilms that utilize polysaccharides as a source of C (Bengtsson et al. 2011; Goecke and Imhoff 2016). The most abundant polysaccharides in brown algae are alginates, cell wall components constituting up to 40% of their dry weight (Painter 1983; Trevathan-Tackett et al. 2015). In a previous study performed in laboratory microcosms we showed that the exudates of *U. pinnatifida*, composed mainly of carbohydrates, induce changes in the structure and function of seawater microbial communities, and also drastically reduce dissolved oxygen levels (Lozada et al. 2021). In particular, incubations with exudates stimulate alginate-degrading capability in the autochtonous seawater bacterial assemblages, and promote the emergence of new bacterial populations (Lozada et al. 2021). Up to now, however, there is a lack of information of bacterial communities associated to *U. pinnatifida* forests during the decay season, and regarding their potential for degrading polysaccharides.

Microbial processing is a key pathway in the C dynamics of coastal food webs, and fundamental due to its potential for C sequestration (Bauer et al. 2013; Zhang et al. 2017; Shen and Benner 2018; Wang 2018). Thus, in order to evaluate the impact of *U. pinnatifida* in environmental C and nutrient budgets and their incorporation in coastal food webs, it is central to consider associated microbial communities, including population dynamics in the epiphytic and free-floating microorganisms within the algal forest and in surface seawater during the algal life cycle. In this work we investigated microbial communities in different environmental compartments of a coastal

site in Patagonia (Punta Este, Golfo Nuevo, Argentina) heavily colonized by *U. pinnatifida*, addressing their structure and potential to degrade alginates. The study focused in the austral spring-summer period at the end of the algae life cycle, when the decaying forest releases massive amounts of organic matter and nutrients to colonized areas, fueling microbial as well as other trophic compartments of coastal food webs.

Materials and Methods

Sampling

Field sampling was performed at Punta Este site, near Puerto Madryn city, in Golfo Nuevo, northern Patagonia, Argentina (42°47′09.47” S, 64°57′30.17” W) (**Figure 1**). Samples were collected in 2019-2020, during the period of senescence and decomposition of *U. pinnatifida* life cycle (from November to March, Casas et al. 2008). Algae sporophytes and seawater samples next to the algal forest (from surface and from bottom inside the forest) were collected concurrently and in triplicate by scuba-diving from a shallow (5 m depth) hard bottom shore (**Figure S1**). Immediately after sample collection, physicochemical parameters [temperature (Temp), salinity (Sal), pH, and dissolved oxygen (DO)] were recorded in each water sample with a multiparameter probe (Aquacomb, HM3070, Trans Instruments, Singapore). Seawater samples were filtered through a plankton mesh (200 µm), poured in acid-washed plastic bottles and transported to the laboratory, thermally insulated and in darkness.

Once in the laboratory, samples were separated and processed for the different analyses. Water samples for the estimation of heterotrophic bacterial (HB) abundance by flow cytometry (Gasol and Morán 2016) were collected as follows: 4 mL samples were directly obtained

from the polypropylene sample containers and fixed with P+G (1% paraformaldehyde + 0.05% glutaraldehyde final concentrations), frozen and stored at −80°C until analysis. For estimation of the alginolytic potential of the microbial community, 5 mL water samples were collected from the containers and analyzed immediately in *in vivo* assays with alginate (see below). For molecular analyses, 100 to 200 mL seawater samples were collected by filtration through 0.2 µm pore size (25 mm diameter) polycarbonate filters (Millipore, Bedford, MA). Epiphytic microbial community samples were collected in sterile swabs by scrubbing ~4 cm^2 of algal blades. Filters and swabs were stored at -80°C until DNA extraction. For the analysis of the dissolved organic carbon (DOC) concentration and quality, and dissolved inorganic carbon (DIC) concentration, 100-mL water samples were filtered in sterile conditions through polyethersulfone membranes (PES, 0.2 µm), and stored in pre-combusted, sterile dark bottles at 4°C. For the analysis of dissolved nutrients, water samples were filtered through 0.2 µm PES membranes, poured in 250 mL acid-washed plastic flasks and frozen immediately.

Algae sporophyte number and dry weight were recorded for each sampling date. The biomass (dry weight per square meter) was calculated by collecting algae sporophytes from 50 x 50 cm quadrants (n=3), and drying the algae at 60°C until constant weight.

Physicochemical analyses

Concentrations of various nutrients [nitrate/nitrite (NO_3+NO_2), ammonium (NH_4), and phosphate (PO_4)] were determined as described after Strickland and Parsons (Strickland and Parsons 1972). Dissolved organic carbon (DOC) concentration was measured using a total C analyzer (TOC-L, Shimadzu) suited with a high-sensitivity catalyzer. The chromophoric and fluorescent fractions of the dissolved organic matter (DOM) pools (CDOM and FDOM,

respectively) were characterized by absorption and fluorescence spectroscopy (Stedmon and Bro 2008). The absorption spectra of filtered seawater samples were measured in a UV-Visible spectrophotometer (Shimadzu UV1800) using a 10 cm pathlength quartz cuvette. Excitation-emission matrices (EEMs) were obtained in a spectrofluorometer (Perkin Elmer LS55) using a 1 cm quartz cuvette.

Heterotrophic bacterial abundance by flow cytometry

For HB determination, 5 µL of a DMSO-diluted SybrGreen I stock (1:100) were added to 500 µL of fixed sample and left for about 10 min in the dark to complete the nucleic acid (NA) staining. Fluorescent beads (yellow-green 1 µm, FluoSpheres Invitrogen) were added (2 µL) as internal standards. Stained samples were run on a FACSCalibur flow cytometer (Becton Dickinson) equipped with a 15 mW blue argon-ion (488 nm) laser and a red laser diode (635 nm). HB populations were detected by their signature in plots of green fluorescence of NA-bound stains (FL1: FITC, 488 nm excitation, 530/30 nm BP emission BP) versus side scatter light (SSC), which is related to the size and granularity of the particles (Gasol et al. 1999). The volume analyzed per sample was estimated considering time, speed (flow rate) and dilution (fixation+beads). The flow rate (µl min^{-1}) was estimated following Gasol and Morán (2016) and HB abundances were calculated accordingly. The analyses of cytometric data were performed with the CellQuest software (Becton Dickinson).

Alginolytic potential assay

Microbial communities collected in different sectors of the *U. pinnatifida* forest were tested *in vivo* for their capability to degrade alginate in laboratory assays. The incubations were perfomed in triplicate, and included the following treatments: a) 600 µL surface seawater samples; b) 600 µL bottom seawater samples (inside the algal forest); and c) a 1 cm^2 disk from the algae lamina (containing epiphytic biofilms) in 600 µL of sterilized seawater. In all cases, 200 µL of 0.2 % (w/v) sodium alginate (Sigma) was added. The controls consisted of 600 µL sterilized seawater plus alginate. Samples were incubated overnight at room temperature. The alginolytic potential of the microbial community was estimated by calculating the increase in absorbance at 235 nm after 24 h (D_A235). This increase relates to the formation of a double bond between C-4 and C-5 at the new non-reducing end of the polysaccharide by the β-elimination reaction catalyzed by alginate lyase enzymes (Cao et al. 2007).

DNA extraction and 16S rRNA gene amplicon sequencing

Filter or swab samples (corresponding to seawater and epiphytic communities, respectively) were resuspended in 1 mL of lysis buffer (400 mM NaCl, 750 mM sucrose, 200 mM EDTA, 50 mM TrisHCl pH 8, Bostrom et al. 2004). DNA was extracted using Fast DNA Spin Kit (MP Biomedicals Inc. USA) following the manufacturer's instructions and was quantified using Hoechst 33258 assay in a fluorometer (QuantiFluor™-ST Fluorometer, Promega, USA). PCR reactions were performed with universal primers spanning the 16S rRNA gene V4 hypervariable region (515F: 5'GTGCCAGCMGCCGCGGTAA' –806R: 5' GGACTACHVGGGTWTCTAAT3' (Apprill et al. 2015; Parada et al. 2016). Sequencing was performed at Genome Québec (Canada).

Bioinformatic and statistical analyses

DOC absorbance data were converted to absorption coefficients (a_λ) following the protocol described by Helms et al. (2008). The absorption coefficient at 440 nm (a_{440}) and the specific absorbance at 254 nm and at 350 nm ($SUVA_{254}$ and $SUVA_{350}$, calculated as aλ/DOC), were used as indicators of aromatic content (Weishaar et al. 2003). The spectral slopes for the intervals 275-295 nm ($S_{275-295}$) and 350-400 nm ($S_{350-400}$) and the slope ratio (S_R= $S_{275-295}/S_{350-400}$) were applied as proxies of molecular weight/size and degradation, with higher S values indicating decreasing molecular weight/size (Helms et al. 2008; Hansen et al. 2016). Fluorescent proxies were calculated from EEMs data. The Freshness index, representing the contribution of OM freshly released into water (β:α , or the ratio of emission intensity at 380 nm divided by the maximum emission intensity between 420 nm and 435 nm at an excitation wavelength of 310 nm), the Humification index, indicative of the presence of humic compounds (HIX, The area under the emission spectra 435–480 nm divided by the peak area 300–345 nm + 435–480 nm, at excitation wavelength of 254 nm) and the Fluorescence index, indicative of the relative contribution of terrestrial and microbial sources (FI, the ratio of emission wavelengths at 470 nm and 520 nm, at an excitation wavelength of 370 nm) (Cory et al., 2005 Huguet et al., 2009, Hansen et al. 2016), were also calculated. Parallel Factor Analysis (PARAFAC)(Bro et al. 2010) was performed to model FDOM fluorescent components from the EEMS, and compared with components modelled in a previous study (Lozada et al. 2021) as well as to the ones listed in the global database OPENFLUOR (Murphy et al. 2014). Multiple Linear Correlation Analysis and Principal Component Analysis (PCA) were applied to select response variables associated with DOC quality. Prior to performing PCA, replicates were averaged and data were standardized to the variance and centered. PCA was performed with the *pca* function included in the FactoMiner package. The analyses were carried out using R 3.2.4 (http://www.R-project.org/).

Two-way ANOVA followed by the Holm-Sidak post hoc test was performed to test for differences in HB abundances between sites and dates. Prior to performing the analyses, the assumptions of normality and homoscedasticity were checked. Significant differences were considered with $P < 0.05$. Analyses were computed with the package SigmaPlot/SigmaStat 12.0.

DNA Sequences were processed with *qiime2* version 2021.4 (Bolyen et al. 2019) using DADA2 to identify amplicon sequence variants (ASV) (Callahan et al. 2016, 2017). ASVs were taxonomically classified in *qiime2* using Greengenes classifier (https://data.qiime2.org/2019.1/common/gg-13-8-99-515-806-nb-classifier.qza). Alpha diversity estimators were calculated in *qiime2* and evaluated for significant differences using Kruskal-Wallis rank sum test followed by multiple comparisons (Dunn test and p-values adjusted with the Bonferroni method). Only samples from dates available for all conditions (November and December) were compared. Taxonomic composition was visualized using barplots and heatmaps at different taxonomic levels with R packages *phyloseq* and *ggplot2*.

Kruskal-Wallis was applied to test for differences among means of D_A235 (alginolytic potential) in the different communities (epiphytic, bottom seawater and surface seawater). *Post-hoc* comparisons were performed applying the Wilcoxon rank sum test with p-values adjusted by the Bonferroni method.

For the comparison of seawater samples, weighted Unifrac similarity index, which takes into account phylogenetic distance among ASVs as well as their relative abundances (McDonald et al. 2018), was used as a distance measure to build matrices for ordinations from the ASV table, and Principal Coordinates Analysis (PCOA) plots were constructed in *qiime2*. A statistical test for partitioning molecular variability in the ASV table among environmental factors (*vegan* R-package, function *adonis2*) was performed. A correspondence analysis (CA) was

performed to a subset of the seawater ASV dataset, constituted by the 200 top abundance ASVs. CA measures the degree of correspondence between the rows and columns (sites and ASVs in this case), this is, how strongly the frequencies deviate from the null model (no association) (Buttigieg and Ramette 2014).

Results

Physicochemical characteristics of seawater

Water temperature and salinity increased steadily during the sampling period, while NO_3+NO_2 showed a decreasing trend **(Table 1)**. Algae dry weight rapidly decreased in the last two months, in agreement with field observations of algae decomposition. Concomitantly, an increase in DOC, NH_4 and PO_4 concentrations was observed near the algal forest (**Table 1, Figure S1**).

The PCA performed to analyze the variation in DOM features through the study period, resulted in three principal components accounting for 88% of total variance (Table S1). The PC1 (46.6 %) correlated positively with the Humification Index (HIX), the two humic-like components C1 (A+M peaks) and C2 (A+C peaks) (Lozada et al. 2021), and the fluorescence index (FI); and correlated negatively with the Freshness index (BIX). Therefore, this first axis can be related to the DOM diagenesis (Figure 2). The PC2 accounted for 26.4% of the total variance; it correlated positively with the a_{440} (also known as water color), and negatively with $S_{275\text{-}295}$ and DIC concentration. This axis can be related to DOM molecular weight/size (MW), as the slope is negatively related to MW, and, together with the increment of the DIC concentration, are signals of

increased microbial degradation of DOM. Finally, the PC3 explained 15.0% of the total variance and correlated positively with DOC concentration (**Table S1**).

Samples from the bottom of the water column inside the algal forest (positioned in negative values of PC1) showed higher Freshness Index and lower HIX (humification), lower values of the humic components C1 and C2 and higher values of the non-humic component C3 **(Figure 2,** "B" samples**)**. These results indicate the fresh nature of organic matter in bottom seawater samples compared to surface water, pointing out inputs from the algal forest. However, the distribution of samples along the PC2 evidenced temporal changes in the algal forest. For example, the large input of decaying biomass observed in January (Figure S1) was coincident with lower values of the $S_{275-295}$, indicating high molecular weight DOM **(Figure 2,** forest samples, B21-01-20**)**. These were also the samples with the highest Freshness index (0.86, Table 1). Although NH_4 concentrations increased with algae decay, following a similar pattern to DOC but with maximum values in January (Figure S1), NH_4 was lower in bottom samples suggesting enhanced nutrient consumption by bacterial respiration within the algal forest **(Figure S1)**. On the other hand, the DIC concentration showed a slight decrease in January, with higher values in the bottom samples (**Figure S2**). Overall, these patterns point to inputs of fresh organic matter by the algal forest with strong influence on microbial activity.

In surface seawater, a delayed but steady transition towards an increase in fresh, high MW organic matter was observed throughout the study period, evidenced by a displacement of surface samples towards negative values of both PC1 and PC2, approaching the positions of the bottom samples (**Figure 2)**. In fact, the relative contribution of the non-humic component C3 (Lozada et al. 2021) increased throughout the sampling period with respect to the humic components C1 and C2, both in bottom and in surface seawater (**Figure S3**).

Microbial communities

Heterotrophic bacteria (HB) abundance

HB abundance fluctuated between $6.4x10^4$ and $6.8x10^5$ cells mL^{-1} with a mean value of $4.68x10^5$ cells mL^{-1} (SD $1.33x10^5$). Two-way ANOVA resulted in statistically significant differences among the HB abundances of different sampling dates (P = 0.006) with higher densities recorded in mid-summer (January), both in surface and bottom water samples (**Figure 3**), coinciding with the increase of fresh organic matter (**Figure 2**, **Figure S1**). Surface and bottom water samples showed similar HB abundances throughout the study period (P = 0.774).

Molecular diversity in the bacterial fraction

Bacterial communities from both surface and bottom seawater (23 samples), as well as epiphytic communities from the algae blades (5 samples), were analyzed by 16S rRNA gene amplicon sequencing. Community structure was analyzed at a cutoff level of 5200 sequences per sample (according to the sample with the lower number of sequences, **Table S2**). At this cutoff level, the diversity indicators were already stabilized, as indicated by the rarefaction curves (**Figure S4**). Overall, 4870 amplicon sequence variants (ASV) were observed within this system. Coverage was higher than 0.990 for all samples (**Table S2**). Diversity indicators are shown in Table 2. The diversity (Shannon's index) showed significant differences among sample types (Kruskal-Wallis H= 9.85, p=0.007). The results of post-hoc comparisons showed that samples from surface and bottom seawater, however, had no significant differences (Kruskal-Wallis H=1.32, corrected P=0.56 . Epiphytic communities, on the other hand, were less diverse than bottom seawater, but no differences were observed with surface seawater (Kruskal-Wallis H=3.1 and 1.9, corrected P=0.005

and 0.18, for bottom and surface, respectively). Estimated richness (Chao1 index) was also lower in epiphytic samples with respect to bottom seawater (Kruskal-Wallis H=3.4, corrected *P*=0.001).

Taxonomic Composition

Even when analyzed at a broad taxonomic level, microbial communities from the different environmental compartments of the studied site were very different, especially the epiphytic community. Typically, members of Archaea constituted 1.2-12.7 % of the sequences in seawater communities, whereas they were not detected in epiphytic communities **(Figure 4, Table S3)**. At the Order level, clear patterns could be observed; for example, among the Gammaproteobacteria, the members of the Order Thiotrichales were much more abundant in epiphytic samples, while Alteromonadales and Oceanospirillales were more prevalent in seawater. The Flavobacteriales (Flavobacteria) were also more abundant in seawater. Among the Archaea, which were only detected in seawater, members of the Thermoplasmata E2 group were detected in all samples, while the Cenarchaeales (Crenarchaeota) were associated with spring (November) samples (Figure **4**). Members of the Saprospirales, Enterobacteriales, Vibrionales, the planctomycetes Pirellulales and Verrucomicrobiales, were exclusively or almost exclusively detected in bottom seawater and epiphytic samples, suggesting that, although epiphytic communities can be considered distinct assemblages, they are related to the algal forest communities (Figure **4**). In addition, differences within epiphytic communities were observed between spring and summer samples, the latter characterized by lower abundances of Thiotrichales and higher of Enterobacteriales (Figure **4**).

A deeper analysis allowed identifying ASVs that were distinctive of epiphytic samples. Different ASVs classified as *Leucothrix* (Gammaproteobacteria, Thiotrichales) were observed, which were very abundant in epiphytic samples and almost absent in seawater (**Figure 5**). A total of 22 ASVs were assigned to *Leucothrix*; together, they accounted for 8 to 56 % of the sequences in epiphytic samples, while they represented less than 3 % in seawater (Table S3). Seven ASVs that could only be assigned to "unclassified Enterobacteriaceae" (Gammaproteobacteria, Enterobacteriales) showed abundances reaching 18% in epiphytic samples (December) samples, but represented less than 3.5% in seawater (Table S3). Lastly, members of the genus *Ralstonia* (Betaproteobacteria, Burkhorderiales) and *Psychromonas* (Gammaproteobacteria, Alteromonadales) were detected, although with lower abundances (**Figure 5**, **Table S3**).

Alginolytic potential

There were marked differences in alginolytic potential among communities, being much higher in epiphytic samples, followed by bottom seawater, and lowest in surface seawater samples (Kruskal-Wallis Test chi-squared – 26.9, $P = 1.4 \times 10^{-06}$, followed by pairwise comparisons using Wilcoxon rank sum test, Figure 6). Higher alginolytic potentials were measured in epiphytic communities particularly in January and March, coinciding with increasing inputs of organic matter from the algae (**Figure 5**). Unfortunately, the number of epiphytic samples (n=5), was too low to allow correlating alginolytic potential with ASV abundances, which could have helped detect alginolytic populations in the dataset.

Beta diversity of seawater microbial communities: relationship with environmental variables

The main sources of variation in seawater communities were identified by Principal Coordinates Analysis based on weighted Unifrac distance. In this case, 17,000 sequences were used as a threshold for rarefaction, corresponding to the seawater sample with the lowest number of sequences (**Table S2**). The results are shown in Figure 7**.** Overall, 79% of the variability was explained by the first three axes. Axis 1 was related with the sampling date and accounted for most of the variability in the samples (52%). On the other hand, Axis 2 (14%) was related with the vertical zonation or depth, showing differences between surface and bottom samples. Notably, January samples showed extreme values along this axis, even those from the surface (Figure 7). Axis 3 (13%) was related to temperature (lower in spring; Table 1), and further separated summer and spring samples along this coordinate.

The distance matrix generated from the seawater ASV table was partitioned among sources of environmental variation, using *adonis2*, a non-parametric multivariate analysis of variance (MANOVA) (Anderson 2001). Season (spring/summer) and sampling zone (bottom/surface), NH_4, NO_3+NO_2, temperature, pH, salinity, and in less extent DO and pH contributed significantly to explain community patterns (Table S4). These results suggest that the structure of bacterial communities was affected by the physicochemical factors coupled tightly with processes occurring in seawater.

We further analyzed the distribution of the top 100 ASV found in seawater, as a function of the ordination pattern of samples, using Correspondence Analysis (CA). This analysis allows detecting the site to species correspondence or the specific site preference (Buttigieg and Ramette 2014). Here, subtler patterns were apparent. For example, among the most abundant ASV, some were typically associated with samples obtained in spring, such as the ones belonging to the Alteromonadales (*Psychromonas* and *Glaciecola*), the Vibrionales (*Pseudoalteromonas*), and some

unclassified Alphaproteobacteria. In addition, the autotrophic *Nitrosopumilus* (Taumarchaeota, Cenarchaeales), capable of oxidizing ammonia, was found predominantly in spring seawater samples. Others, such as some ASV belonging to Archaea (Thermoplasmata, Marine group II) were distributed along the axis with summer samples, indicating these taxa are more frequent in summer. Members of the Rhodobacterales, such as *Loktanella*, *Octadecabacter* and *Thalassobius*, and of the Flavobacteriales (*Polaribacter*, *Tenacibaculum*) were positioned in the center, indicating that they are frequent members of these communities, regardless of their spatial and temporal differences. The position of ASVs from Thiotrichales (very common in epiphytic communities, see previous sections) corresponded to late summer samples affected by the massive transfer of senescent algae biomass to seawater (Figure S6).

Discussion

The impact of the invasive kelp *Undaria pinnatifida* in heavily colonized coastal environments of Patagonia is expected to peak in summer, due to the high biomass attained and its massive decay during summer months. In this work, we analyzed physicochemical and microbial aspects associated with the life cycle of *U. pinnatifida* in Punta Este (northeastern Patagonia) focusing on changes associated with biomass release during its annual decay. Algal biomass was found to peak in December (~700 g m^{-2}), decreasing rapidly afterwards, with a concomitant increase in seawater DOC concentration. Biomass values recorded in this work were much higher than previous records obtained at the same site in 2006 (November, 440 g m^{-2} , Rechimont et al. 2013), suggesting an increasing trend in the density of *U. pinnatifida* forest in this coastal ecosystem. According to estimations from previous work, *U. pinnatifida* releases an average of 0.1 mg C L^{-1} day^{-1} into seawater, similar to other kelp species (Lozada et al. 2021). Moderate DOC values (1.5 - 2 mg L^{-1}) recorded in seawater in Punta Este in this work, even at the end of summer period when large inputs of senescent biomass are incorporated in the system, suggest that there are efficient mechanisms of algal-derived DOC turnover and/or export, which likely control DOC levels with implications for the C cycle in this coastal area.

The release of DOM from the algal biomass into the seawater could be tracked throughout the study period, influencing DOC concentration and seawater quality. This process was clearly driven by the algal forest and affected surface seawater with a temporal delay relative to the algal decay, indicative of some level of DOM export. Moreover, regeneration-derived nutrients (NH_4 and PO_4) also increased concomitantly, indicating nutrient inputs from biomass, either directly from algae or indirectly from other organisms benefiting from algae through the trophic web or from habitat generation. Whereas NO_3+NO_2 followed the usual pattern observed in

temperate enclosed coastal areas. These gulfs, and particularly Nuevo Gulf, show lower macronutrients availability in summer compared to winter levels when mixing events bring nutrients back to the euphotic zone promoting spring blooms (Solis 1998; Williams et al. 2018).

Higher DIC and lower NH_4 concentrations were observed in the bottom with respect to surface seawater, suggesting enhanced C and nutrient consumption by microbial respiration in seawater inside the forest. As kelps can be an important source of N for seawater (Yoshikawa et al. 2001), the results suggest a highly active microbial community associated with the algal forest. These results are in line with a previous microcosm study, in which the labile carbon compounds released by algal exudates increased microbial abundance and processing triggering changes in DOC quality characterized by signals of freshness and microbial degradation (Lozada et al. 2021). The significant amounts of DOC contributed by macroalgae are a major C source for microbial communities, fueling the microbial loop (Wada et al. 2008; Reed et al. 2015; Pfister et al. 2019). As a result of this process, microorganisms incorporate biomass at the base of the food web cascading to higher trophic levels. Concomitantly, refractory DOC is produced, in a process known as "microbial carbon pump", recognized to be relevant to explain C sequestration in the ocean (Jiao et al. 2011). However, the amounts of DOC as well as the proportion of labile to refractory DOC released by macroalgae are dependent on a number of factors including seaweed species and environmental conditions. Up to now it is unclear to what extent seaweed-derived DOC results in a net sink of atmospheric CO_2 and thus significantly contribute to carbon sequestration (Paine et al. 2021).

Although in this work we did not evaluate levels of particulate organic carbon (POC), an important liberation of particles was observed in the algal forest during the summer period, concomitant to a sharp biomass decrease. Large amounts of algae particles were evident to the

naked eye and contributed to seawater turbidity. Studies carried out in aquaculture facilities have shown that *U. pinnatifida* biomass erosion can reach 80% during algal decay (Yoshikawa et al. 2001). Although *U. pinnatifida* contributes to the POC pool through liberation of particles during senescence, it could also have a role in C sequestration through biomass production and export. The role of *U. pinnatifida* in enhancing net primary production, resulting in a net gain in carbon production and export, has been shown (Tait et al. 2015), however, information about the export process restrict to the drifting of biomass ashore in summer (Bunicontro et al. 2019). Studies performed in *Laminaria hyperborea* showed that up 98% of the biomass may be exported as particles (Smale et al. 2021). The process is complex, and can involve interactions at multiple levels. For example, shredders such as sea urchins consume a high percentage of kelp detritus, accelerating C export through faeces (Filbee-Dexter et al. 2020). Both urchins and snails have been observed to feed on *U. pinnatifida* at the study site of this work (Punta Este) in Patagonia (Teso et al. 2009) and DNA sequences from this algal species were found in stomachs from the invasive green crab *Carcinus maenas* in a nearby site in Nuevo Gulf (Cordone et al. 2020). On the other hand, the higher abundance of grazers associated with *U. pinnatifida* could have a negative impact on other algae beyond *U. pinnatifida* growth season, through increased pressure resulting in the depletion of other C sources (Dumes, Kate 2016). The balance between all these processes will probably determine the ultimate impact of this exotic species in the coastal C cycle, taking into account that macroalgal forests are now starting to be considered in the context of blue carbon (Krause-Jensen et al. 2018; Filbee-Dexter and Wernberg 2020).

Bacterial communities were characterized by their abundance (flow cytometry), their diversity/structure (16S rRNA gene amplicon sequencing) and their capability to degrade the main polysaccharide of *U. pinnatifida* (*in vivo* alginate degradation assays). Seawater microbial patterns were tightly coupled to seawater characteristics and processes. For example, community structure

was associated with the sampling date, season (spring *vs.* summer) and origin (surface *vs.* bottom seawater samples inside the algal forest), as well as with other key physicochemical indicators such as nutrients. Alginate degradation potential was higher in forest water samples than in surface seawater. Heterotrophic bacterial abundance increased in summer, when the algae biomass decreased after peaking in December and fresh DOC was being released. Clasen and Shurin (2015), in a work focusing on Canadian kelp forests with various algae of the order Laminariales, observed that larger forests produced more detritus and DOM, which stimulated microbial communities, specifically alginate lyase-carrying microorganisms, increasing alginate lyase potential in seawater (Clasen and Shurin 2015). Our results from coastal environments of Patagonia indicate that the communities from the bottom, inside the algal forest, are different and more diverse than the ones from surface water. These results are in accordance with other works showing distinct microbial communities with higher taxonomic and phylogenetic diversity in kelp beds (Pfister et al. 2019).

Epiphytic communities from *U. pinnatifida* blades were very particular in terms of structure and function, including the presence of distinct ASVs with high microdiversity. These communities also had a much higher alginolytic potential than those of seawater, suggesting a high level of specialization and an active role in the degradation process of *U. pinnatifida* biomass. As regards their structure, epiphytic communities showed lower diversity and different composition compared to seawater, although they shared many taxa with the bottom seawater samples. Kelp forest-enriched taxa were also found to be shared on *Nereocystis luetkeana* or *Macrocystis pyrifera* blades (Pfister et al. 2019). Moreover, it has been shown that host species identity, geographic location, and blade tissue age influence the structure of microbial communities on canopy-forming kelps (Weigel and Pfister 2019). These characteristics could be indicating a recruitment and selection of bacterial populations from seawater performing specific functions (Egan et al. 2013). In addition, we found the dominant ASVs from epiphyte communities to be enriched in seawater

samples from later dates, suggesting a two-way exchange, the recruitment from seawater and the transference from epiphytic communities to seawater during the massive algae decay period.

The 16S rRNA gene-based community structure analysis allowed identifying a number of bacterial genera that provide clues regarding the ecosystem functions of these communities. For example, various populations of the genus *Leucothrix* (Gammaproteobacteria, Thiotrichales) were observed associated with algal blades, and together accounted for a large fraction of epiphytic communities. These are well known filamentous epiphytic bacteria, that feed on the algae biomass rather than on carbon sources from seawater, and occurring mostly in temperate environments (Brock 1966; Bland and Brock 1973). More recently, these bacteria were found associated with changes in seawater quality due to large-scale aquaculture of seaweeds in coastal regions in China (Xie et al. 2017). *Pseudoalteromonas* (Gammaproteobacteria, Vibrionales) were abundant in seawater, mainly from the bottom seawater in the algal forest, and also found in epiphytic communities. These heterotrophic bacteria are highly specialized, capable of degrading various types of complex organic matter, and producing a wide range of extracellular enzymes, including enzymes that degrade algal polysaccharides (Bowman 2007; Lee et al. 2016; Gobet et al. 2018). They are aerobic, motile, and secrete biologically active compounds, which makes them good candidates for the colonization of algal particles in seawater, a fundamental process for POM turnover in the marine environment (Holmström and Kjelleberg 1999; Grossart et al. 2003). *Psychromonas* and *Glaciecola* (Gammaproteobacteria, Alteromonadales) are two psychrotrophs, which displayed higher abundances in spring when water temperatures were still low. The autotrophic *Nitrosopumilus* (Taumarchaeota, Cenarchaeales), capable of oxidizing ammonia to nitrate (Könneke et al. 2005), was found in spring samples. This archaeon, thought to be key both to C and N cycling in the ocean, is adapted to nutrient limitation due to its extremely high affinity for ammonium, and uses a novel and very efficient carbon fixation pathway (Könneke et al. 2014). On

the other hand, the marine group II Archaea were very abundant and diverse. These are widespread members of seawater occurring also in polar regions, comprising mainly heterotrophs or photoheterotrophs (Santoro et al. 2019; Rinke et al. 2019). They prefer the photic zone and show high diversity in coastal waters with pronounced seasonal variations (Zhang et al. 2015).

Concluding remarks

In this work, we uncovered changes in relevant physicochemical and microbial characteristics related to the presence of a high biomass of the invasive kelp *U. pinnatifida* in a coastal environment in Patagonia. The process of biomass decomposition was accompanied by changes in seawater, including changes in the DOC quantity and quality, in the structure of microbial communities, and in specific microbial functions related to algal polysaccharide degradation. In addition to common seawater bacterial and archaeal taxa, specific bacterial populations of epiphytic lifestyle were identified. In particular, a relationship between epiphytic and seawater communities from the algal forest was evident, suggesting that the microorganisms on the algal blades are themselves a source of these populations for the surrounding seawater and viceversa. Further studies are in progress involving the analysis of seawater and the role of benthic microbial communities in the degradation of algal biomass in an annual cycle in the Atlantic Patagonian coast.

References

Anderson, M. J. 2001. A new method for non-parametric multivariate analysis of variance. Austral Ecol. **26**, 32–46. doi:10.1111/j.1442-9993.2001.01070.pp.x

Apprill, A., S. McNally, R. Parsons, and L. Weber. 2015. Minor revision to V4 region SSU rRNA 806R gene primer greatly increases detection of SAR11 bacterioplankton. Aquat. Microb. Ecol. **75**, 129–137. doi:10.3354/ame01753

Arnosti, C., M. Wietz, T. Brinkhoff, J.-H. Hehemann, D. Probandt, L. Zeugner, and R. Amann. 2021. The biogeochemistry of marine polysaccharides: sources, inventories, and bacterial drivers of the carbohydrate cycle. Annu. Rev. Mar. Sci. **13**, 81–108. doi:10.1146/annurev-marine-032020-012810

Bauer, J. E., W.-J. Cai, P. A. Raymond, T. S. Bianchi, C. S. Hopkinson, and P. A. G. Regnier. 2013. The changing carbon cycle of the coastal ocean. Nature **504**, 61–70. doi:10.1038/nature12857

Bland, J. A., and T. D. Brock. 1973. The marine bacterium *Leucothrix mucor* as an algal epiphyte. Mar. Biol. **23**, 283–292. doi:10.1007/BF00389315

Bengtsson, M.M., Sjøtun, K., Storesund, J.E., Øvreås, L., 2011. Utilization of kelp-derived carbon sources by kelp surface-associated bacteria. Aquat. Microb. Ecol. **62**, 191-199. https://doi.org/10.3354/ame01477

Bolyen, E., J. R. Rideout, M. R. Dillon, and others. 2019. Reproducible, interactive, scalable and extensible microbiome data science using QIIME 2. Nat. Biotechnol. **37**, 852–857. doi:10.1038/s41587-019-0209-9

Boström, K. H., K. Simu, A. Hagström, and L. Riemann. 2004. Optimization of DNA extraction for quantitative marine bacterioplankton community analysis. Limnol. Oceanogr. Methods **2**, 365–373. doi:10.4319/lom.2004.2.365

Bowman, J. P. 2007. Bioactive compound synthetic capacity and ecological significance of marine bacterial genus *Pseudoalteromonas*. Mar. Drugs **5**, 220–241.

Bro, R., N. Viereck, M. Toft, H. Toft, P. I. Hansen, and S. B. Engelsen. 2010. Mathematical chromatography solves the cocktail party effect in mixtures using 2D spectra and PARAFAC. TrAC Trends Anal. Chem. **29**, 281–284. doi:10.1016/j.trac.2010.01.008

Brock, T.D., 1966. The habitat of *Leucothrix mucor*, a widespread marine microorganism. Limnol. Oceanogr. **11**, 303–307. https://doi.org/10.4319/lo.1966.11.2.0303

Bunicontro, M. P., S. C. Marcomini, and G. N. Casas. 2019. Environmental impacts of an alien kelp species (*Undaria pinnatifida*, Laminariales) along the patagonian coasts, p. 373–396. *In* C. Makowski and C.W. Finkl [eds.], Impacts of Invasive Species on Coastal Environments: Coasts in Crisis. Springer International Publishing.

Buttigieg, P. L., and A. Ramette. 2014. A guide to statistical analysis in microbial ecology: a community-focused, living review of multivariate data analyses. FEMS Microbiol. Ecol. **90**, 543–550. doi:10.1111/1574-6941.12437

Callahan, B. J., P. J. McMurdie, and S. P. Holmes. 2017. Exact sequence variants should replace operational taxonomic units in marker-gene data analysis. ISME J. **11**, 2639–2643. doi:10.1038/ismej.2017.119

Callahan, B. J., P. J. McMurdie, M. J. Rosen, A. W. Han, A. J. A. Johnson, and S. P. Holmes. 2016. DADA2: High resolution sample inference from Illumina amplicon data. Nat. Methods **13**, 581–583. doi:10.1038/nmeth.3869

Cao, L., L. Xie, X. Xue, H. Tan, Y. Liu, and S. Zhou. 2007. Purification and characterization of alginate lyase from streptomyces species strain A5 isolated from banana rhizosphere. J. Agric. Food Chem. **55**, 5113–5117. doi:10.1021/jf0704514

Casas, G., R. Scrosati, and M. L. Piriz. 2004. The invasive kelp *Undaria pinnatifida* (Phaeophyceae, Laminariales) reduces native seaweed diversity in Nuevo Gulf (Patagonia, Argentina). Biol. Invasions **6**, 411–416.

Casas, G.N., Piriz, M.L., Parodi, E.R., 2008. Population features of the invasive kelp *Undaria pinnatifida* (Phaeophyceae: Laminariales) in Nuevo Gulf (Patagonia, Argentina). Journal of the Marine Biological Association of the United Kingdom **88**, 21–28. https://doi.org/10.1017/S0025315408000246

Clasen, J. L., and J. B. Shurin. 2015. Kelp forest size alters microbial community structure and function on Vancouver Island, Canada. Ecology **96**, 862–872. doi:10.1890/13-2147.1

Cordone, G., M. Lozada, E. Vilacoba, B. Thalinger, G. Bigatti, D. A. Luitmaer, D. Steinke, and D. E. Galván. 2021. Metabarcoding, direct stomach observation and stable isotope analysis reveal a highly diverse diet for the invasive green crab in Atlantic Patagonia. Biol. Invasions **24**, 505-526. doi:10.1007/s10530-021-02659-5

Cory, R.M., McKnight, D.M., 2005. Fluorescence spectroscopy reveals ubiquitous presence of oxidized and reduced quinones in dissolved organic matter. Environ. Sci. Technol. **39**, 8142–8149. https://doi.org/10.1021/es0506962

Dellatorre, F. G., R. O. Amoroso, J. Saravia, and J. M. Orensanz. 2014. Rapid expansion and potential range of the invasive kelp *Undaria pinnatifida* in the southwestern Atlantic. Aquatic Invasions **9,** 467–478. doi:10.3391/ai.2014.9.4.05

Deniaud-Bouët, E., N. Kervarec, C. Michel, T. Tonon, B. Kloareg, and C. Hervé. 2014. Chemical and enzymatic fractionation of cell walls from Fucales: insights into the structure of the extracellular matrix of brown algae. Ann. Bot. **114**, 1203–1216. doi:10.1093/aob/mcu096

Duarte, C. M., J. Wu, X. Xiao, A. Bruhn, and D. Krause-Jensen. 2017. Can seaweed farming play a role in climate change mitigation and adaptation? Front. Mar. Sci. **4**, 100. doi:10.3389/fmars.2017.00100

Egan, S., T. Harder, C. Burke, P. Steinberg, S. Kjelleberg, and T. Thomas. 2013. The seaweed holobiont: understanding seaweed–bacteria interactions. FEMS Microbiol. Rev. **37**, 462–476. doi:10.1111/1574-6976.12011

Epstein, G., and D. A. Smale. 2017. *Undaria pinnatifida*: A case study to highlight challenges in marine invasion ecology and management. Ecol. Evol. **7**, 8624–8642. doi:10.1002/ece3.3430

Fieler, R., M. Greenacre, S. Matsson, L. Neves, S. Forbord, and K. Hancke. 2021. Erosion dynamics of cultivated kelp, *Saccharina latissima*, and implications for environmental management and carbon sequestration. Front. Mar. Sci. **8**, 1573. doi:10.3389/fmars.2021.632725

Filbee-Dexter, K., M. F. Pedersen, S. Fredriksen, K. M. Norderhaug, E. Rinde, T. Kristiansen, J. Albretsen, and T. Wernberg. 2020. Carbon export is facilitated by sea urchins transforming kelp detritus. Oecologia **192**, 213–225. doi:10.1007/s00442-019-04571-1

Filbee-Dexter, K., and T. Wernberg. 2020. Substantial blue carbon in overlooked Australian kelp forests. Sci. Rep. **10**, 12341. doi:10.1038/s41598-020-69258-7

Gasol, J. M., and X. A. G. Morán. 2016. Flow cytometric determination of microbial abundances and its use to obtain indices of community structure and relative activity, p. 159–187. *In* T.J. McGenity, K.N. Timmis, and B. Nogales [eds.], Hydrocarbon and Lipid Microbiology Protocols: Single-Cell and Single-Molecule Methods. Springer.

Gasol, J. M., U. L. Zweifel, F. Peters, J. A. Fuhrman, and Å. Hagström. 1999. Significance of size and nucleic acid content heterogeneity as measured by flow cytometry in natural planktonic bacteria. Appl. Environ. Microbiol. **65**, 4475–4483.

Gobet, A., T. Barbeyron, M. Matard-Mann, G. Magdelenat, D. Vallenet, E. Duchaud, and G. Michel. 2018. Evolutionary evidence of algal polysaccharide degradation acquisition by *Pseudoalteromonas carrageenovora* 9T to adapt to macroalgal niches. Front. Microbiol. **9**, 2740. doi:10.3389/fmicb.2018.02740

Goecke, F. R., and J. F. Imhoff. 2016. Microbial biodiversity associated with marine macroalgae and seagrasses, p. 3–25. *In* E. Olafsson [ed.], Marine Macrophytes as Foundation Species. CRC Press, Boca Raton, FL.

Grossart, H.-P., T. Kiørboe, K. Tang, and H. Ploug. 2003. Bacterial colonization of particles: growth and interactions. Appl. Environ. Microbiol. **69**, 3500–3509. doi:10.1128/AEM.69.6.3500-3509.2003

Hansen, A. M., T. E. C. Kraus, B. A. Pellerin, J. A. Fleck, B. D. Downing, and B. A. Bergamaschi. 2016. Optical properties of dissolved organic matter (DOM): Effects of biological and photolytic degradation. Limnol. Oceanogr. **61**, 1015–1032. doi:10.1002/lno.10270

Hardison, A., E. Canuel, I. Anderson, and B. Veuger. 2010. Fate of macroalgae in benthic systems: carbon and nitrogen cycling within the microbial community. Mar. Ecol. Prog. Ser. **414**, 41–55. doi:10.3354/meps08720

Helms, J. R., A. Stubbins, J. D. Ritchie, E. C. Minor, D. J. Kieber, and K. Mopper. 2008. Absorption spectral slopes and slope ratios as indicators of molecular weight, source, and photobleaching of chromophoric dissolved organic matter. Limnol. Oceanogr. **53**, 955–969.

Holmström, C., and S. Kjelleberg. 1999. Marine *Pseudoalteromonas* species are associated with higher organisms and produce biologically active extracellular agents. FEMS Microbiol. Ecol. **30**, 285–295. doi:10.1111/j.1574-6941.1999.tb00656.x

Huguet, A., Vacher, L., Relexans, S., Saubusse, S., Froidefond, J. M., & Parlanti, E. 2009. Properties of fluorescent dissolved organic matter in the Gironde Estuary. Organic Geochemistry **40,** 706-719. doi: 10.1016/j.orggeochem.2009.03.002

Irigoyen, A. J., G. Trobbiani, M. P. Sgarlatta, and M. P. Raffo. 2011. Effects of the alien algae *Undaria pinnatifida* (Phaeophyceae, Laminariales) on the diversity and abundance of benthic macrofauna in Golfo Nuevo (Patagonia, Argentina): potential implications for local food webs. Biol. Invasions **13**, 1521–1532. doi:10.1007/s10530-010-9910-9

James, Kate. 2016. A review of the impacts from invasion by the introduced kelp *Undaria pinnatifida*. Technical Report 2016/40 Report: TR 2016/40. Report: TR 2016/40 Waikato Regional Council.

Jiao, N., G. J. Herndl, D. A. Hansell, and others. 2011. The microbial carbon pump and the oceanic recalcitrant dissolved organic matter pool. Nat. Rev. Microbiol. **9**, 555.

Könneke, M., A. E. Bernhard, J. R. de la Torre, C. B. Walker, J. B. Waterbury, and D. A. Stahl. 2005. Isolation of an autotrophic ammonia-oxidizing marine archaeon. Nature **437**, 543–546. doi:10.1038/nature03911

Könneke, M., D. M. Schubert, P. C. Brown, and others. 2014. Ammonia-oxidizing archaea use the most energy-efficient aerobic pathway for CO_2 fixation. Proc. Natl. Acad. Sci. **111**, 8239–8244. doi:10.1073/pnas.1402028111

Krause-Jensen, D., and C. M. Duarte. 2016. Substantial role of macroalgae in marine carbon sequestration. Nat. Geosci. **9**, 737–742. doi:10.1038/ngeo2790

Krause-Jensen, D., P. Lavery, O. Serrano, N. Marbà, P. Masque, and C. M. Duarte. 2018. Sequestration of macroalgal carbon: the elephant in the Blue Carbon room. Biol. Lett. **14**, 20180236. doi:10.1098/rsbl.2018.0236

Krumhansl, K. A., and R. E. Scheibling. 2012. Production and fate of kelp detritus. Mar. Ecol. Prog. Ser. **467**, 281–302. doi:10.3354/meps09940

Lee, S.-H., H. Choe, S.-G. Kim, D.-S. Park, A. Nasir, B. K. Kim, and K. M. Kim. 2016. Complete genome of brown algal polysaccharides-degrading *Pseudoalteromonas issachenkonii* KCTC 12958T (=KMM 3549T). J. Biotechnol. **219**, 86–87. doi:10.1016/j.jbiotec.2015.12.031

Lozada, M., M. C. Diéguez, P. E. García, G. Bigatti, J. P. Livore, E. Giarratano, M. N. Gil, and H. M. Dionisi. 2021. *Undaria pinnatifida* exudates trigger shifts in seawater chemistry and

microbial communities from Atlantic Patagonian coasts. Biol. Invasions **23,** 1781–1801. doi:10.1007/s10530-021-02471-1

Matos, M. N., M. Lozada, L. E. Anselmino, and others. 2016. Metagenomics unveils the attributes of the alginolytic guilds of sediments from four distant cold coastal environments. Environ. Microbiol. **18**, 4471–4484. doi:10.1111/1462-2920.13433

McDonald, D., Y. Vázquez-Baeza, D. Koslicki, J. McClelland, N. Reeve, Z. Xu, A. Gonzalez, and R. Knight. 2018. Striped UniFrac: enabling microbiome analysis at unprecedented scale. Nat. Methods **15**, 847–848. doi:10.1038/s41592-018-0187-6

Murphy, K. R., Stedmon, C. A., Wenig, P., and R. Bro. 2014. OpenFluor– an online spectral library of auto-fluorescence by organic compounds in the environment. Analytical Methods, **6**, 658-661.

Paine, E.R., Schmid, M., Boyd, P.W., Diaz-Pulido, G., Hurd, C.L., 2021. Rate and fate of dissolved organic carbon release by seaweeds: A missing link in the coastal ocean carbon cycle. Journal of Phycology **57**, 1375–1391. https://doi.org/10.1111/jpy.13198

Painter, T. J. 1983. 4 - Algal Polysaccharides, p. 195–285. *In* G.O. Aspinall [ed.], The Polysaccharides. Academic Press.

Parada, A. E., D. M. Needham, and J. A. Fuhrman. 2016. Every base matters: assessing small subunit rRNA primers for marine microbiomes with mock communities, time series and global field samples. Environ. Microbiol. **18**, 1403–1414. doi:10.1111/1462-2920.13023

Pedersen, M. F., K. Filbee-Dexter, K. M. Norderhaug, S. Fredriksen, N. L. Frisk, C. W. Fagerli, and T. Wernberg. 2020. Detrital carbon production and export in high latitude kelp forests. Oecologia **192**, 227–239. doi:10.1007/s00442-019-04573-z

Pfister, C. A., M. A. Altabet, and B. L. Weigel. 2019. Kelp beds and their local effects on seawater chemistry, productivity, and microbial communities. Ecology **100**, e02798. doi:10.1002/ecy.2798

Rechimont, M. E., D. E. Galván, M. C. Sueiro, and others. 2013. Benthic diversity and assemblage structure of a north Patagonian rocky shore: a monitoring legacy of the NaGISA project. J. Mar. Biol. Assoc. U. K. **93**, 2049–2058. doi:10.1017/S0025315413001069

Reed, D. C., C. A. Carlson, E. R. Halewood, J. C. Nelson, S. L. Harrer, A. Rassweiler, and R. J. Miller. 2015. Patterns and controls of reef-scale production of dissolved organic carbon by giant kelp *Macrocystis pyrifera*. Limnol. Oceanogr. **60**, 1996–2008. doi:10.1002/lno.10154

Rinke, C., F. Rubino, L. F. Messer, and others. 2019. A phylogenomic and ecological analysis of the globally abundant Marine Group II Archaea (Ca. Poseidoniales ord. nov.). ISME J. **13**, 663–675. doi:10.1038/s41396-018-0282-y

Santoro, A. E., R. A. Richter, and C. L. Dupont. 2019. Planktonic marine Archaea. Annu. Rev. Mar. Sci. **11**, 131–158. doi:10.1146/annurev-marine-121916-063141

Shen, Y., and R. Benner. 2018. Mixing it up in the ocean carbon cycle and the removal of refractory dissolved organic carbon. Sci. Rep. **8**, 2542. doi:10.1038/s41598-018-20857-5

Smale, D. A., A. Pessarrodona, N. King, and P. J. Moore. 2021. Examining the production, export, and immediate fate of kelp detritus on open-coast subtidal reefs in the Northeast Atlantic. Limnol. Oceanogr. doi:10.1002/lno.11970

Solis, M. E. 1998. Monitoring in Nuevo Gulf (Argentina): analysis of oceanographic data by geographic information systems (GIS). Master Thesis. International Institute for Infraestructural, Hydraulic and Environmental Engineering (IHE) – Delft, Netherland.

South, P. M., O. Floerl, B. M. Forrest, and M. S. Thomsen. 2017. A review of three decades of research on the invasive kelp *Undaria pinnatifida* in Australasia: An assessment of its success, impacts and status as one of the world's worst invaders. Mar. Environ. Res. **131**, 243–257. doi:10.1016/j.marenvres.2017.09.015

Stedmon, C. A., and R. Bro. 2008. Characterizing dissolved organic matter fluorescence with parallel factor analysis: a tutorial. Limnol. Oceanogr. Methods **6**, 572–579. doi:10.4319/lom.2008.6.572

Strickland, J. D. H., and T. R. Parsons. 1972. A practical handbook of seawater analysis, Fisheries Research Board of Canada.

Tait, L. W., P. M. South, S. A. Lilley, M. S. Thomsen, and D. R. Schiel. 2015. Assemblage and understory carbon production of native and invasive canopy-forming macroalgae. J. Exp. Mar. Biol. Ecol. **469**, 10–17. doi:10.1016/j.jembe.2015.04.007

Teso, V., G. Bigatti, G. Casas, M. L. Piriz, and P. Penchaszadeh. 2009. Do native grazers from Patagonia, Argentina, consume the invasive kelp *Undaria pinnatifida*? Rev. Mus. Argent. Cienc. Nat. Nueva Ser. **11**, 7-14–14.

Trevathan-Tackett, S. M., J. Kelleway, P. I. Macreadie, J. Beardall, P. Ralph, and A. Bellgrove. 2015. Comparison of marine macrophytes for their contributions to blue carbon sequestration. Ecology **96**, 3043–3057. doi:10.1890/15-0149.1

Wada, S., M. N. Aoki, A. Mikami, T. Komatsu, Y. Tsuchiya, T. Sato, H. Shinagawa, and T. Hama. 2008. Bioavailability of macroalgal dissolved organic matter in seawater. Mar. Ecol. Prog. Ser. **370**, 33–44. doi:10.3354/meps07645

Wada, S., and T. Hama. 2013. The contribution of macroalgae to the coastal dissolved organic matter pool. Estuar. Coast. Shelf Sci. **129**, 77–85. doi:10.1016/j.ecss.2013.06.007

Wang, L. 2018. Microbial control of the carbon cycle in the ocean. Natl. Sci. Rev. **5**, 287–291. doi:10.1093/nsr/nwy023

Watanabe, K., G. Yoshida, M. Hori, Y. Umezawa, H. Moki, and T. Kuwae. 2020. Macroalgal metabolism and lateral carbon flows can create significant carbon sinks. Biogeosciences **17**, 2425–2440. doi:10.5194/bg-17-2425-2020

Weishaar, J. L., G. R. Aiken, B. A. Bergamaschi, M. S. Fram, R. Fujii, and K. Mopper. 2003. Evaluation of specific ultraviolet absorbance as an indicator of the chemical composition and reactivity of dissolved organic carbon. Environ. Sci. Technol. **37**, 4702–4708. doi:10.1021/es030360x

Williams, G. N., M. E. Solís, and J. L. Esteves. 2018. Satellite-measured phytoplankton and environmental factors in North Patagonian gulfs, p. 307–325. *In* M.S. Hoffmeyer, M.E. Sabatini, F.P. Brandini, D.L. Calliari, and N.H. Santinelli [eds.], Plankton Ecology of the Southwestern Atlantic: From the Subtropical to the Subantarctic Realm. Springer International Publishing.

Weigel, Brooke L., and Pfister, C.A. 2019. Successional dynamics and seascape-level patterns of microbial communities on the canopy-forming kelps *Nereocystis luetkeana* and *Macrocystis pyrifera*. Frontiers in Microbiology **10**, 346. https://www.frontiersin.org/article/10.3389/fmicb.2019.00346.

Weigel, B.L., and Pfister, C.A. 2021. The dynamics and stoichiometry of dissolved organic carbon release by kelp. Ecology **102**, e03221. https://doi.org/10.1002/ecy.3221

Xie, X., Z. He, X. Hu, H. Yin, X. Liu, and Y. Yang. 2017. Large-scale seaweed cultivation diverges water and sediment microbial communities in the coast of Nan'ao Island, South China Sea. Sci. Total Environ. **598**, 97–108. doi:10.1016/j.scitotenv.2017.03.233

Yoshikawa, T., I. Takeuchi, and K. Furuya. 2001. Active erosion of *Undaria pinnatifida* Suringar (Laminariales, Phaeophyceae) mass-cultured in Otsuchi Bay in northeastern Japan. J. Exp. Mar. Biol. Ecol. **266**, 51–65. doi:10.1016/S0022-0981(01)00346-X

Zhang, C. L., W. Xie, A.-B. Martin-Cuadrado, and F. Rodriguez-Valera. 2015. Marine Group II Archaea, potentially important players in the global ocean carbon cycle. Front. Microbiol. **6**, 1108. doi:10.3389/fmicb.2015.01108

Zhang, Y., M. Zhao, Q. Cui, and others. 2017. Processes of coastal ecosystem carbon sequestration and approaches for increasing carbon sink. Sci. China Earth Sci. **60**, 809–820. doi:10.1007/s11430-016-9010-9

Tables

Table 1. Main physicochemical parameters of seawater samples from Punta Este (Nuevo Gulf, Patagonia, Argentina). Values are means (standard deviation). S: surface, B: bottom, in the algal forest. T: Temperature, Sal: salinity, DO: dissolved oxygen, DOC: dissolved organic carbon concentration, DIC: dissolved inorganic carbon concentration, NO_3^- + NO_2^-: dissolved nitrates + nitrites, NH_4^+: ammonium ion, PO_4^{3+}: orthophosphate ion.

	Nov		**Dec**		**Jan**		**Mar**	
	S	**B**	**S**	**B**	**S**	**B**	**S**	**B**
T (°C)	13.7 (0.0)	14.6 (0.4)	16.9 (0)	16.9 (0.1)	19.3 (0.2)	19.2 (0.1)	19.5 (0.5)	19.6 (0.1)
Sal (ppt)	33.0 (0.1)	32.7 (0.1)	32.0 (0.1)	32.0 (0.1	33.8 (0.1)	33.8 (0.1)	34.2 (0.1)	34.1 (0.1)
pH	8.0 (0.0)	7.9 (0.1)	8.1 (0.0)	7.9 (0.1)	8.4 (0.1)	8.3 (0.0)	8.0 (0.0)	8.1 (0.0)
DO (%)	90 (2.0)	69.0 (7.9)	97 (0)	96 (3)	95 (2)	94 (1)	86 (1)	98 (1)
DOC (mg L^{-1})	1.0 (0.2)	1.2 (0.2)	1.1 (0.1)	1.1 (0.1)	0.99 (0.0)	1.3 (0.1)	1.5 (0.6)	1.9 (na)
DIC (mg L^{-1})	25.5 (0.1)	25.9 (0.7)	25.1 (0.4)	26.7 (0.2)	24.2 (1.4)	25.7 (0.1)	25.2 (0.6)	26.5 (na)
NH_4 (µM)	0.5 (0.2)	0.4 (0.1)	0.2 (0.0)	0.2 (0.1)	1.6 (0.1)	0.8 (0.1)	0.8 (0.2)	0.7 (0.2)
NO_3+NO_2 (µM)	1.1 (0.4)	1.2 (0.6)	0 (0)	0 (0)	0.2 (0.1)	0.2 (0)	0.3 (0.1)	1.0 (0.1)
PO_4 (µM)	1.0 (0.1)	1.1 (0.0)	0.9 (0.0)	0.9 (0.0)	2.4 (0.1)	2.1 (0.2)	2.2 (0.1)	2.1 (0.1)

BIX	0.81 (0.25)	0.94 (0.03)	0.73 (0.35)	0.91 (0.03)	0.93 (0.06)	0.96 (0.20)	0.87 (0.03)	0.94 (NA)
FI	2.00 (0.30)	1.94 (0.01)	1.99 (0.619)	1.74 (0.21)	1.82 (0.09)	1.72 (0.04)	1.77 (0.07)	2.00 (NA)
HIX	4.53 (2.54)	3.18 (0.38)	4.08 (2.90)	2.84 (0.09)	3.05 (0.35)	2.61 (1.17)	2.58 (0.41)	4.53 (NA)
S(275-295)	0.025 (0.001)	0.025 (0.001)	0.024 (0.001)	0.024 (0.001)	0.022 (0.003)	0.023 (0.003)	0.023 (0.001)	0.024 (NA)
a_{440}	0.08 (0.03)	0.05 (0.02)	0.10 (0.02)	0.06 (0.00)	0.09 (0.02)	0.10 (0.08)	0.10 (0.01)	0.08 (NA)
$SUVA_{254}$	2.44 (0.54)	2.18 (0.34)	2.69 (0.14)	2.38 (0.29)	2.38 (0.54)	2.43 (0.58)	2.19 (0.60)	1.68 (NA)
a_{350}:DOC	0.35 (0.06)	0.27 (0.06)	0.42 (0.14)	0.29 (0.00)	0.38 (0.08)	0.33 (0.19)	0.31 (0.04)	0.27 (NA)

na: not applicable (less than 3 values)

Table 2. Diversity indicators of microbial communities from Punta Este. Values are shown as average (SD). Nseqs: number of sequences per sample. Nseqs_r: number of sequences after rarefaction (for details, see Materials and Methods).

Community	**Nseqs**	**nseqs_r**	**Observed ASVs**	**Good's Coverage**	**Chao1 Richness**	**Shannon's Diversity**	**Pielou's Evenness**
Seawater-surface (n=11)	42,548 (5880)	5200 (0)	224 (51)	0.995 (0.002)	239 (55)	6.2 (0.5)	0.80 (0.05)
Seawater-forest (n=12)	36,258 (9966)	5200 (0)	262 (67)	0.995 (0.002)	276 (71)	6.7 (0.4)	0.84 (0.03)
Epiphytic (n=5)	10,867 (7364)	5200 (0)	121 (26)	0.999 (0.001)	122 (28)	5.3 (0.5)	0.77 (0.06)

Figure Legends

Figure 1. Sampling location (Punta Este, black dot) in Nuevo gulf, Patagonia, Argentina.

Figure 2. Principal Components Analysis considering DOM features of seawater samples from different compartments of a *U. pinnatifida* forest (Punta Este, Nuevo Gulf, Patagonia, Argentina). A- PC1 vs. PC2. B- PC1 vs. PC3. Due to high variability among samples, the analysis of the average of three biological replicates is shown. Points are named as: bottom (B) or surface (S), followed by the sampling date (dd-mm-yy).

Figure 3. Abundance of heterotrophic bacteria estimated by flow cytometry in seawater samples from different compartments of *U. pinnatifida* forest in Punta Este (n=3 for each boxplot).

Figure 4. A- Taxonomic composition of microbial communities from Punta Este, summarized at the Order level. Empty spaces correspond to low abundance (less than 1.5%) groups. Samples are named as "PE" followed by the sampling date (dd/mm), sample type (S: surface, B; bottom, E: epiphytic) and replicate number (1 to 3). The complete ASV table with its taxonomic classification can be found in Supplementary Material (Table S3).

Figure 5. Heatmap showing the samples and their ASV abundances. Only the 100 more abundant ASV (ASVs with abundances across samples among the top 100) were plotted. Numbers correspond to the taxonomic assignment for each ASV. Key: 1- *Polaribacter* sp., 2- Candidatus

Portiera, 3- Thermoplasmata Marine group II, 4- unclassified Flavobacteriaceae, 5- unclassified Alphaproteobacteria, 6- *Synechococcus* sp., 7- unclassified Rhodobacteraceae, 8- *Thalassobius* sp., 9-Alteromonadales OM60, 10- *Octadecabacter* sp., 11- *Tenacibaculum* sp., 12- *Glaciecola* sp., 13-unclassified Methylophylaceae, 14- *Loktanella* sp., 15- unclassified Cryomorphaceae, 16-unclassified Bacteria, 17- *Pseudoalteromonas* sp., 18-unclassified Methylophylaceae, 19-Acidimicrobiales OCS155, 20- unclassified Oceanospirillales, 21- *Nitrosopumilus* sp., 22-*Psychromonas* sp., 23-*Thiomicrospira* sp., 24- *Leucothrix* sp., 25- unclassified Enterobacteriaceae, 26- unclassified Gammaproteobacteria, 27- *Ralstonia* sp., 28- *Propionigenium* sp. 29- unclassified Oceanospirillaceae, 30- unclassified Cryomorphaceae, 31- Alteromonadaceae HTCC2207. ASVs were assigned to taxa with the Naive Bayesian classifier trained on the Greengenes 13_8 99% OTUs database, available as a qiime2 plugin. Complete taxonomic assignments are available in Supplementary Material (Table S3).

Figure 6. Alginolytic potential in bacterial communities from *U. pinnatifida* forest in Punta Este. D_A235: difference in absorbance at 235 nm, measured in overnight incubations with sodium alginate. Letters correspond to significant differences between mean values (n=12 for each condition). Note the logarithmic scale of the y axis.

Figure 7. Principal Coordinates Analysis ordination of seawater communities from Punta Este, based on Weighted Unifrac distance matrix. The threshold for rarefaction was 17,000 sequences, corresponding to the seawater sample with less sequences (PE_0303_B1, **Table S2**). Analyses were performed in *qiime2*. The samples from the same sampling date(above plot) or season (below plot) are grouped with ellipses.

Figure 1

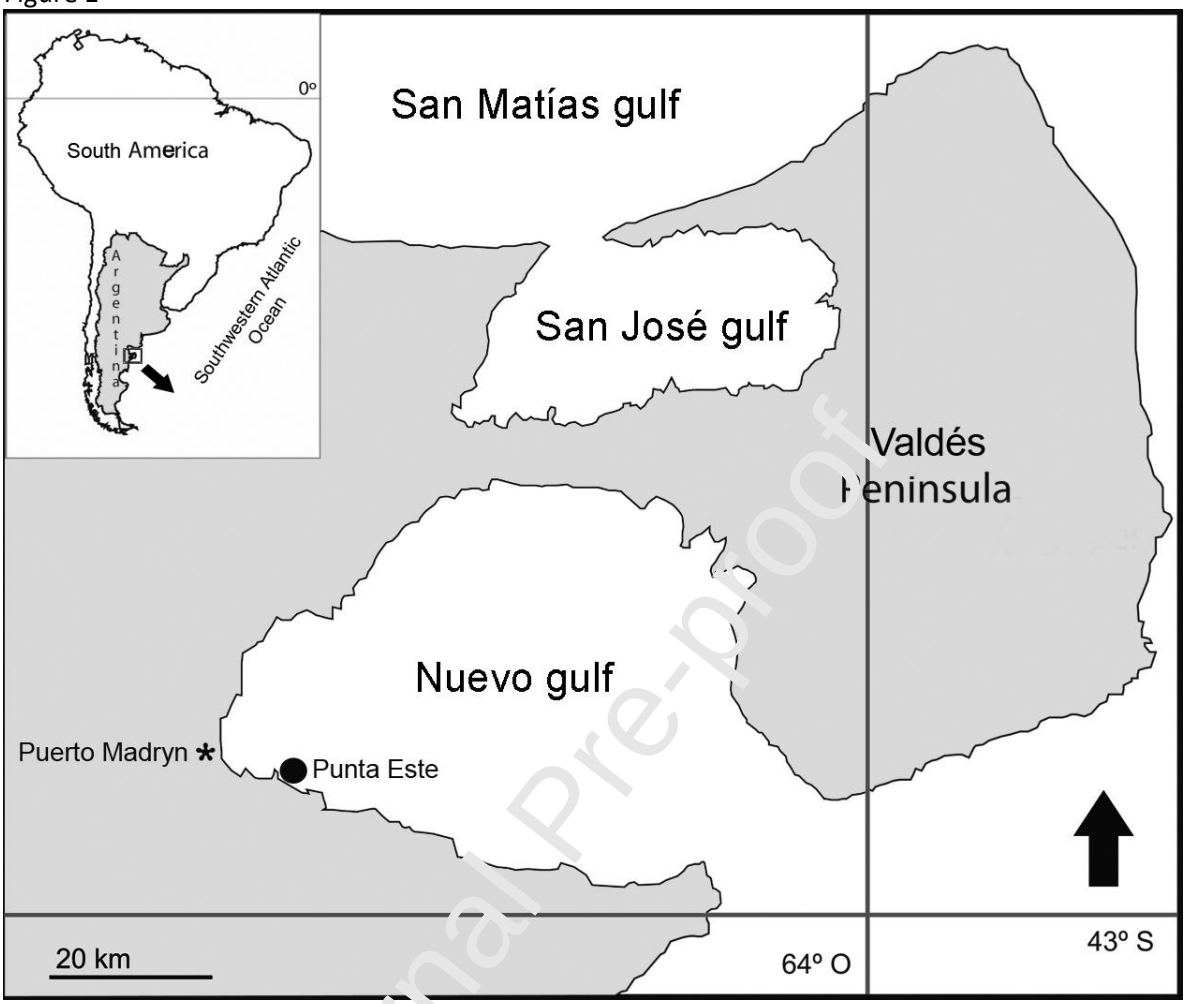

Figure 2

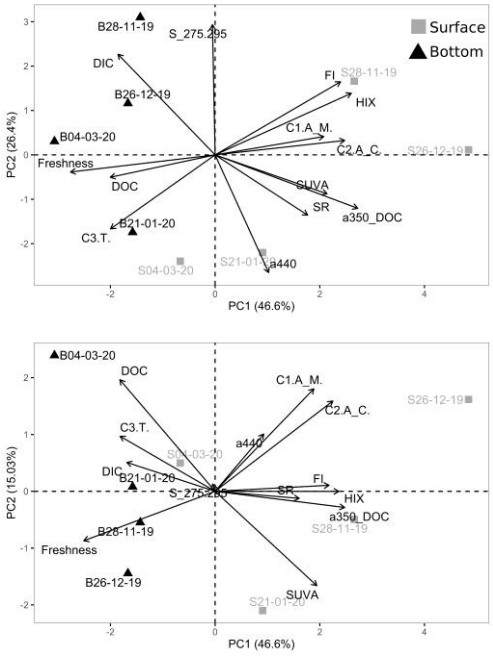

Figure 3

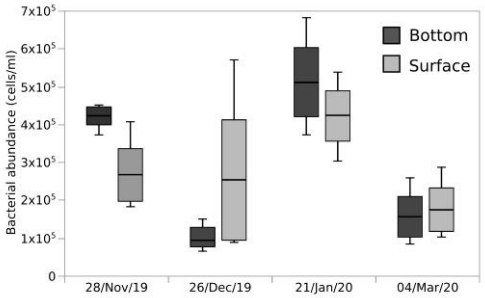

Figure 4

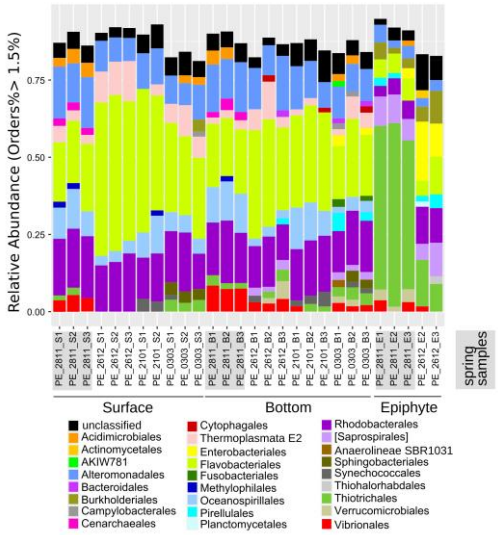

Figure 5

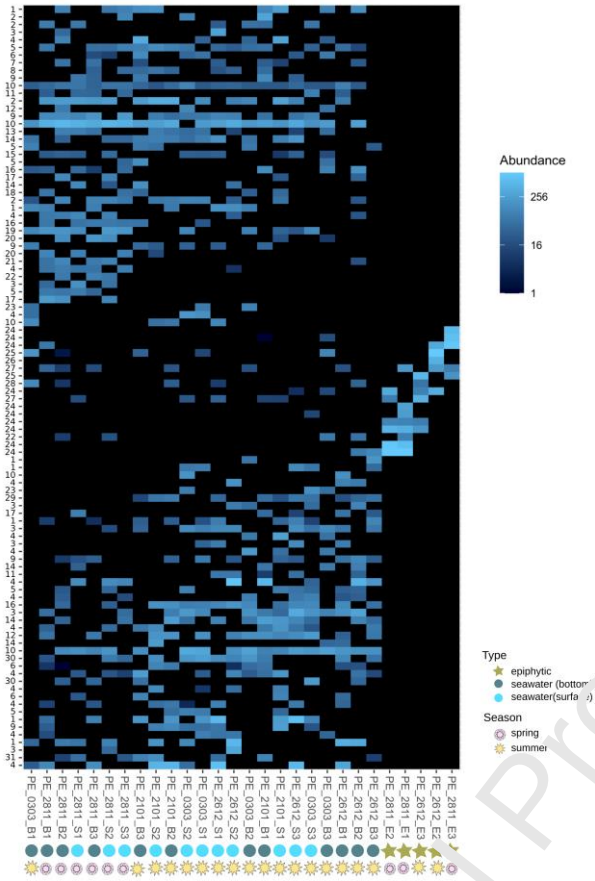

Figure 6

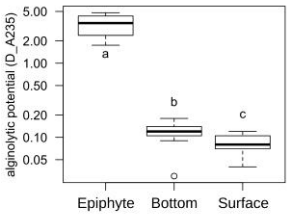

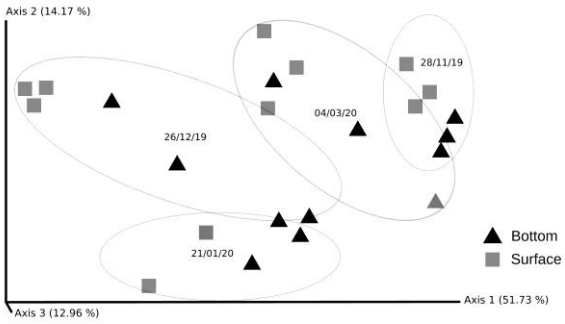

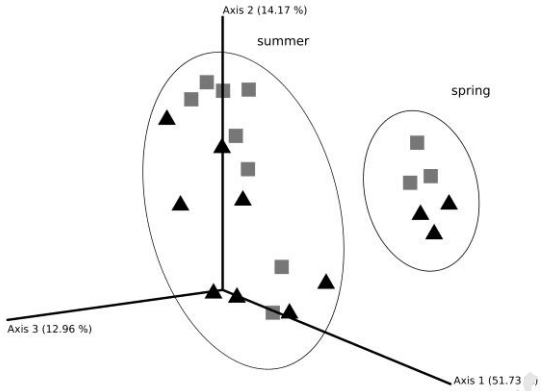

Figure 7

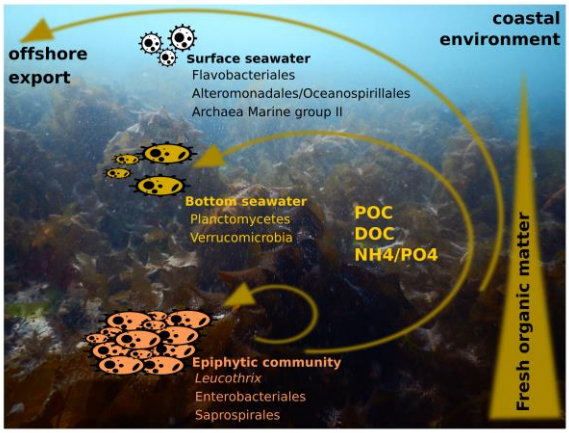

Graphical Abstract